

Electronic Supplementary Information

Iron-Catalysed Atom Transfer Radical Polyaddition for the Synthesis and Modification of Novel Aliphatic Polyesters Displaying Lower Critical Solution Temperature and pH- Dependent Release Behaviors

*Yu-Chi Lu, Li-Chieh Chou and Chih-Feng Huang**

Department of Chemical Engineering, National Chung Hsing University, 145 Xingda Road, Taichung
402, Taiwan

Captions of ESI

Experiments.

Table S1. Estimated (Est.) and MALDI-TOF MS experimental (Exp.) m/z values of the linear type
PVBBPA polyester (entry 9 in Table 1: $M_n = 3461$; $D = 1.90$).

Scheme S1. Possible side reactions and resulting chemical structures during ATRPA of VBBPA.

Figure S1. ^1H NMR spectrum (400 MHz, CDCl_3) of PVBBPA [entry 5, Table 1 ($M_w = 26,810$; $D = 1.50$)].

Figure S2. ATRPA performed with various iron catalysts at 70 °C: (a) FeBr_3 and (b) FeCl_3
[VBBPA/ $\text{FeX}_3 = 500/1$ (entries 7 and 8 in Table 1)].

Figure S3. GPC traces of the products of the ATRPA of VBBPA performed using various temperatures
and reducing agents.

Figure S4. FT-IR spectra (3900–500 cm^{-1}) of (a) PVBBPA and (b) PVBAPA.

Figure S5. (A1, B1) ^1H NMR (400 MHz, CDCl_3) and (A2, B2) FT-IR (3900–500 cm^{-1}) spectra of (A1, A2) $\text{OEG}_7\text{-OH}$ and (B1, B2) $\text{OEG}_7\text{-}\equiv$.

Figure S6. GPC traces recorded (a) before and (b) after the click reactions of the PVBAPAs with $\text{OEG}_7\text{-}\equiv/\text{Oct}$ at various feeding ratios, affording APBs.

Figure S7. SEM morphologies of APBs featuring various grafting compositions of OEG_7/Oct [(a) 100/0 and (b) 76/24].

Figure S8. Plots of the intensity ratios (I_{392}/I_{372}) in the fluorescence spectra of the APBs with respect to the concentration, probed using pyrene molecules, to determine their CMCs.

Figure S9. Monitoring the stability of micelles in different pH values and times in RT by DLS.

Experiments

Synthesis of 4-vinylbenzyl 2-bromo-2-phenylacetate (VBBPA). 4-Vinylbenzyl alcohol was synthesized from 4-vinylbenzyl chloride according to previous reports^{1, 2} [yield 92%; ^1H NMR (400 MHz, CDCl_3 , δ/ppm): 4.64 (s, PhCH_2 , 2H), 5.25 and 5.76 (d, $\text{CH}_2=\text{CH}$, 2H), 6.68–6.75 (dd, $\text{CH}_2=\text{CH}$, 1H), 7.29–7.41 (m, C_6H_4 , 4H)]. For the synthesis of VBBPA, a 500-mL two-neck round-bottomed flask was dried and refilled with N_2 . VBA (9.4 g, 70 mmol), α -bromophenylacetic acid (15 g, 70 mmol), and dry CH_2Cl_2 (200 mL) were charged into the flask. A solution of 4-dimethylaminopyridine (0.85 g, 2.0 mmol) and N,N' -dicyclohexylcarbodiimide (14.4 g, 70.0 mmol) in dry CH_2Cl_2 (50 mL)

was added dropwise to the flask with stirring at 0 °C for a few hours. The temperature of the mixture was elevated to 40 °C, where it was maintained for an additional 24 h under N₂. The solids were filtered off; the filtrate was washed with 1 M HCl_(aq), 1 M NaOH_(aq), and water and then dried (MgSO₄). After evaporation of the solvents, the residue was purified through column chromatography [SiO₂; EtOAc/hexane, 1:10 (v/v)] to give a yellowish liquid {yield: 78%; ¹H NMR (400 MHz, CDCl₃, δ = ppm): 5.20 (dd, PhCH₂, 2H), 5.28 and 5.75 (d, CH₂=CH, 2H), 5.40 [s, PhCH(C=O)Br, 1H], 6.68–6.75 (dd, CH₂=CH, 1H), 7.27–7.40 and 7.51 (m, C₆H₄ and C₆H₅, 9H)}.

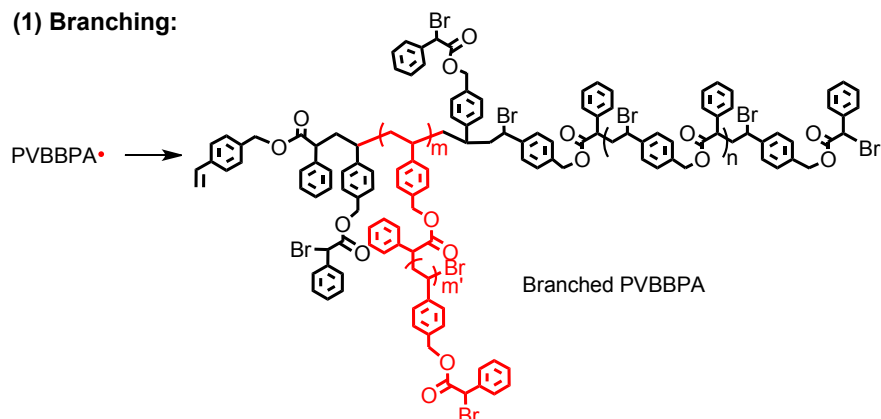
Synthesis of OEG_n–≡. A general example for OEG₇–≡: A 250-mL round-bottom flask was charged with OEG₇–OH (8.33 g, 40.0 mmol), NaH₂ (2.30 g, 96.0 mmol), and anhydrous THF (100 mL). Propargyl bromide (6.89 mL, 80.0 mmol) was added dropwise to the mixture, cooled in an ice bath, over 60 min and then the mixture was vigorously stirred for another 24 h at RT. The reaction was stopped by adding de-ionized water; the aqueous phase was extracted with CH₂Cl₂. The combined organic extracts were dried (MgSO₄) and concentrated under vacuum. The product was dried in a vacuum oven {yield: 78%; ¹H NMR (400 MHz, CDCl₃, δ = ppm): 4.22 (s, -OCH₂C≡CH, 2H), 3.65 [m, (CH₂CH₂O)₇, 4H], 3.50 (s, OCH₃, 3H), and 2.44 (s, OCH₂C≡CH, 1H)}. The ¹H NMR and FT-IR spectra are presented in Figure S5.

Table S1. Estimated (Est.) and MALDI-TOF MS experimental (Exp.) m/z values of the linear type PVBBPA polyester (entry 9 in Table 1: $M_n = 3461$; $D = 1.90$).

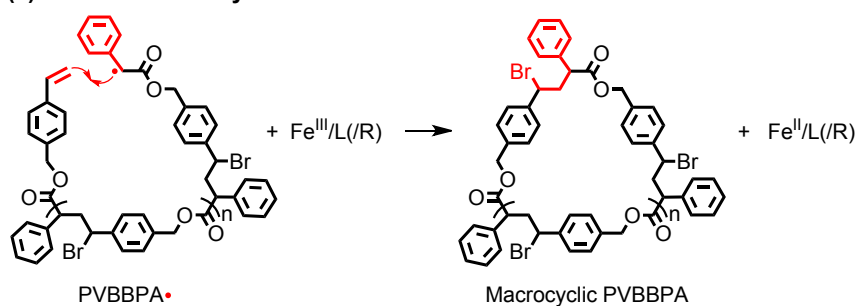
Original linear type chemical formula	$C_{17}H_{15}O_2(C_{17}H_{15}BrO_2)_{x-1}C_{17}H_{15}BrO_2Br$		
Leaving group during MALDI-TOF	$-C_9H_9O_2^*$	$-C_9H_9O_2^* \& -Br$	$-C_9H_9O_2^* \& -C_8H_5BrO^*$
Detected formula in Figure S3	$C_8H_6(C_{17}H_{15}BrO_2)_xBr$ (▲ series)	$C_8H_6(C_{17}H_{15}BrO_2)_x^*$ (● series)	$C_8H_6(C_{17}H_{15}BrO_2)_xC_9H_{10}BrO$ (■ series)
m/z values x values	Est. / Exp.	Est. / Exp.	Est. / Exp.
x= 1	513.25 / 513.41	—	—
x= 2	844.86 / 844.82	764.55 / 764.08	647.43 / 648.26
x= 3	1175.67 / 1176.34	1095.76 / 1094.95	978.64 / 978.93
x= 4	1506.88 / 1507.12	1426.97 / 1426.41	—
x= 5	1838.08 / 1838.10	1758.18 / 1756.68	—
x= 6	2169.29 / 2168.90	2089.39 / 2089.14	—
x= 7	2500.25 / 2500.32	2420.60 / 2420.22	—

Scheme S1. Possible side reactions and resulting chemical structures during ATRPA of VBBPA.

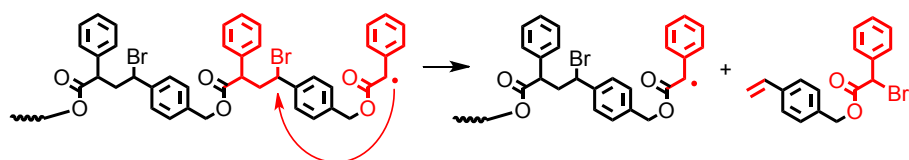
(1) Branching:



(2) Intramolecular cycloaddition:



(3) β -scission:



(4) Intermolecular crosslinking:

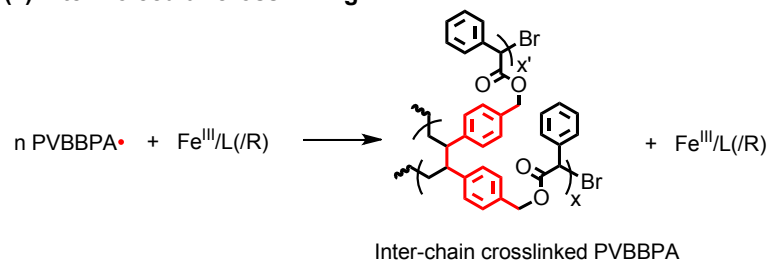


Figure S1. ^1H NMR spectrum (400 MHz, CDCl_3) of PVBBPA [entry 5, Table 1 ($M_w = 26,810$; $\bar{D} = 1.50$)].

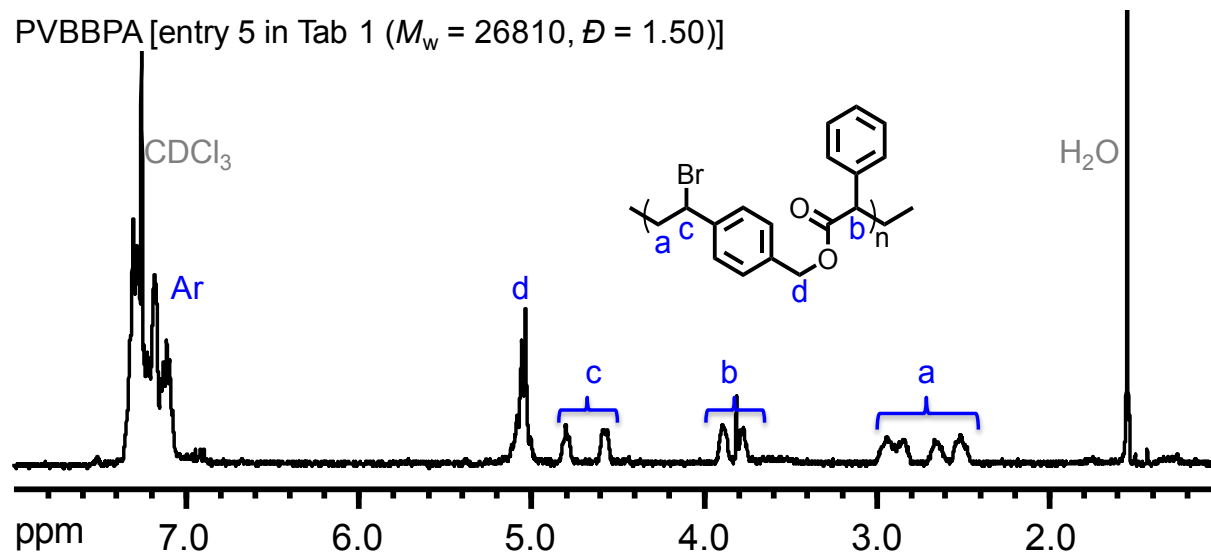


Figure S2. ATRPA performed with various iron catalysts at 70 °C: (a) FeBr₃ and (b) FeCl₃ [VBBPA/FeX₃ = 500/1 (entries 7 and 8 in Table 1)].

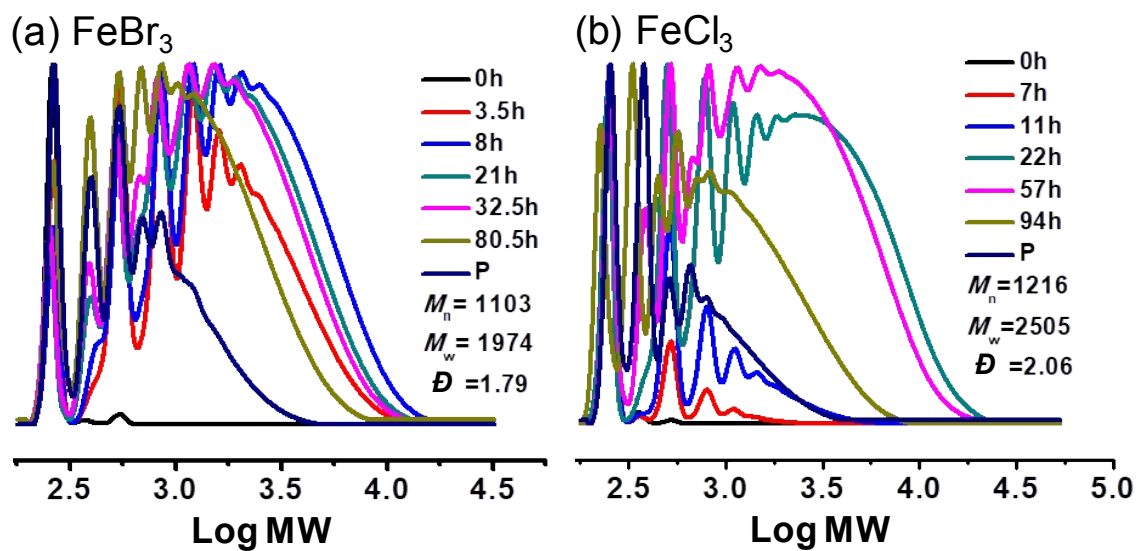


Figure S3. GPC traces of the products of the ATRPA of VBBPA performed using various temperatures and reducing agents.

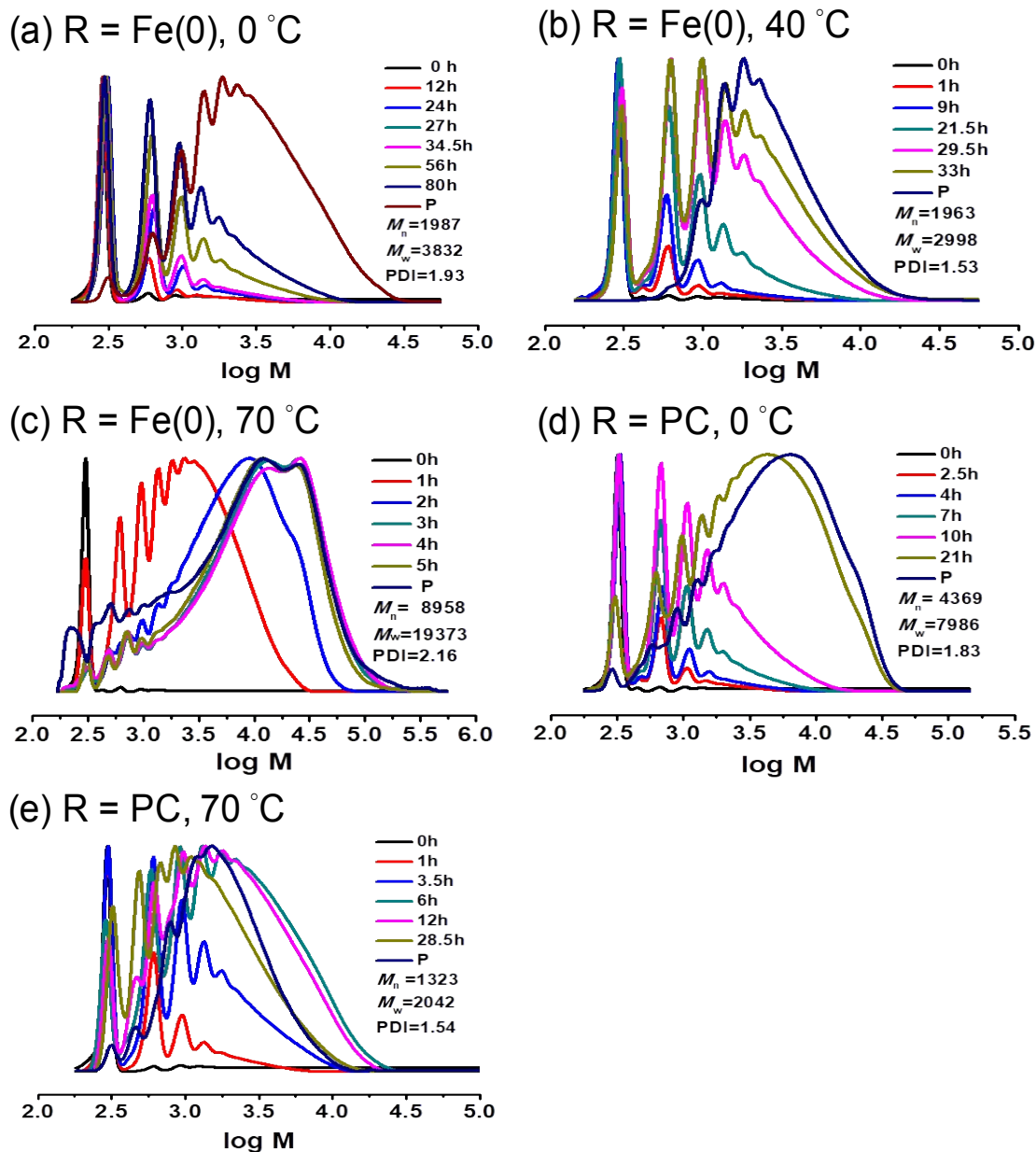


Figure S4. FT-IR spectra (3900–500 cm^{-1}) of (a) PVBBPA and (b) PVBAPA.

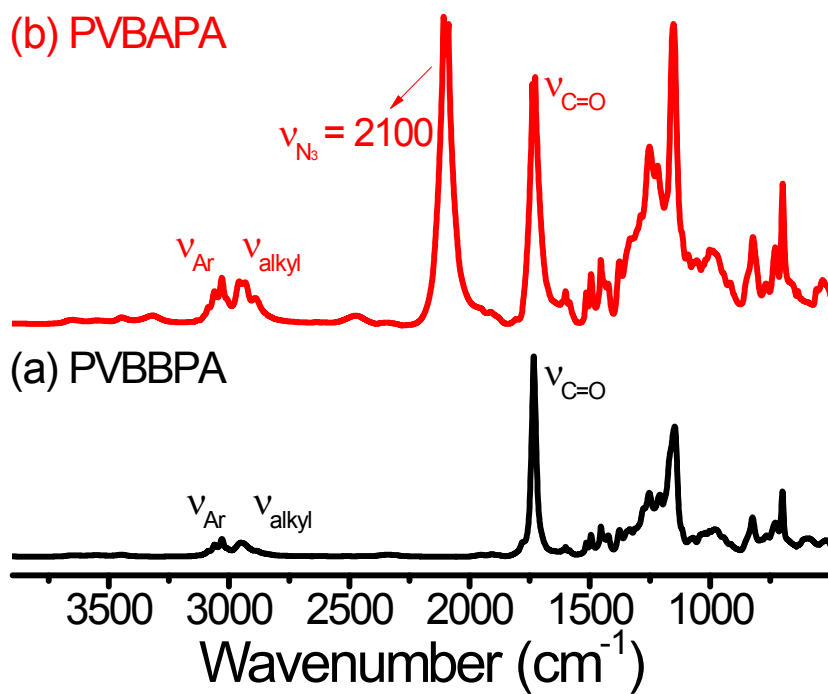


Figure S5. (A1, B1) ^1H NMR (400 MHz, CDCl_3) and (A2, B2) FT-IR (3900–500 cm^{-1}) spectra of (A1, A2) OEG₇-OH and (B1, B2) OEG₇-≡.

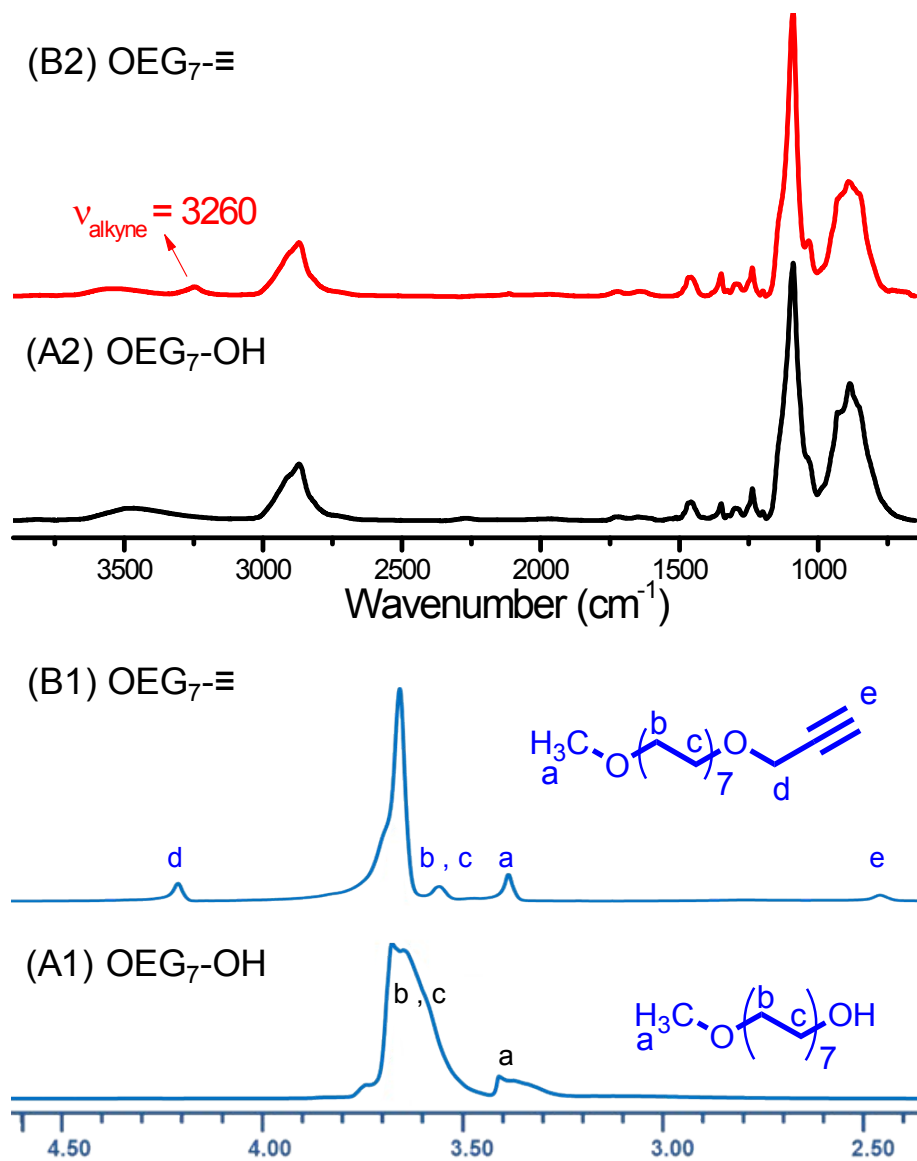


Figure S6. GPC traces recorded (a) before and (b) after the click reactions of the PVBAPAs with OEG₇-≡/Oct at various feeding ratios, affording APBs.

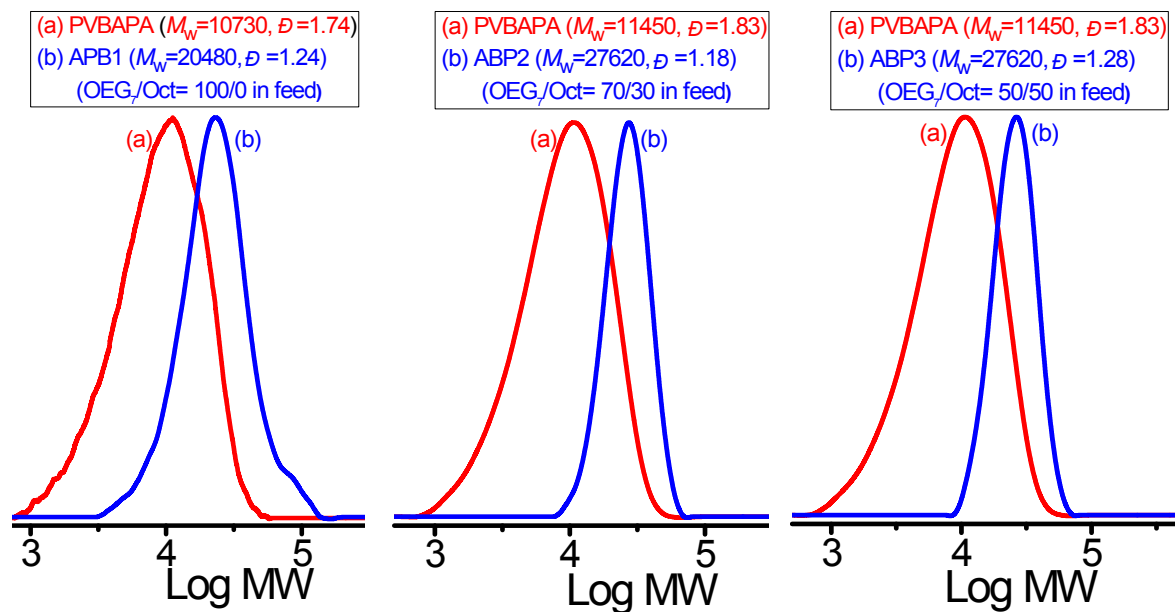


Figure S7. SEM morphologies of APBs featuring various grafting compositions of OEG₇/Oct [(a) 100/0 and (b) 76/24].

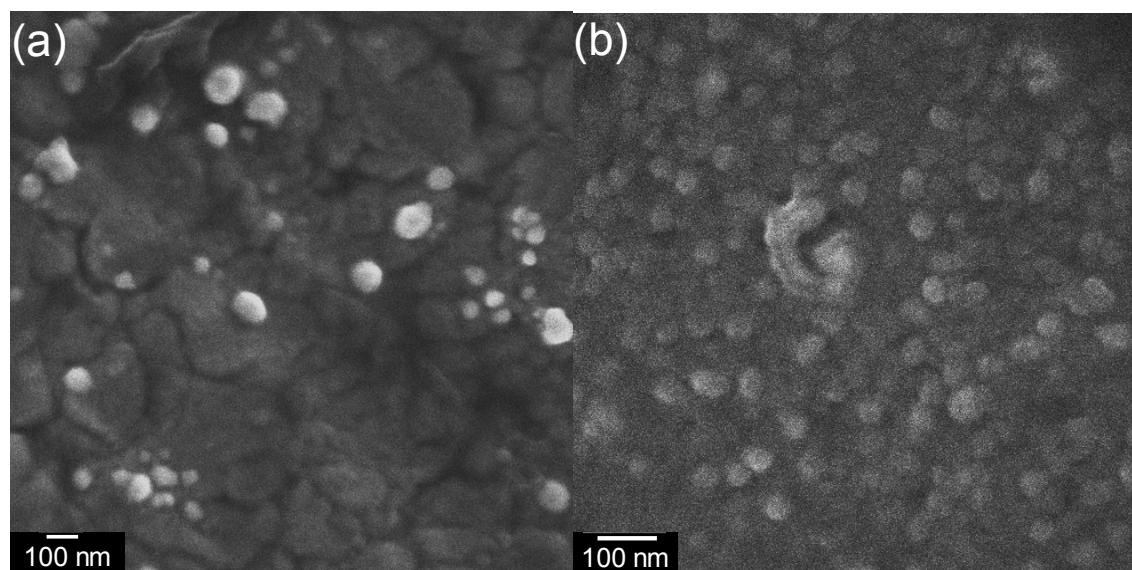


Figure S8. Plots of the intensity ratios (I_{392}/I_{372}) in the fluorescence spectra of the APBs with respect to the concentration, probed using pyrene molecules, to determine their CMCs.

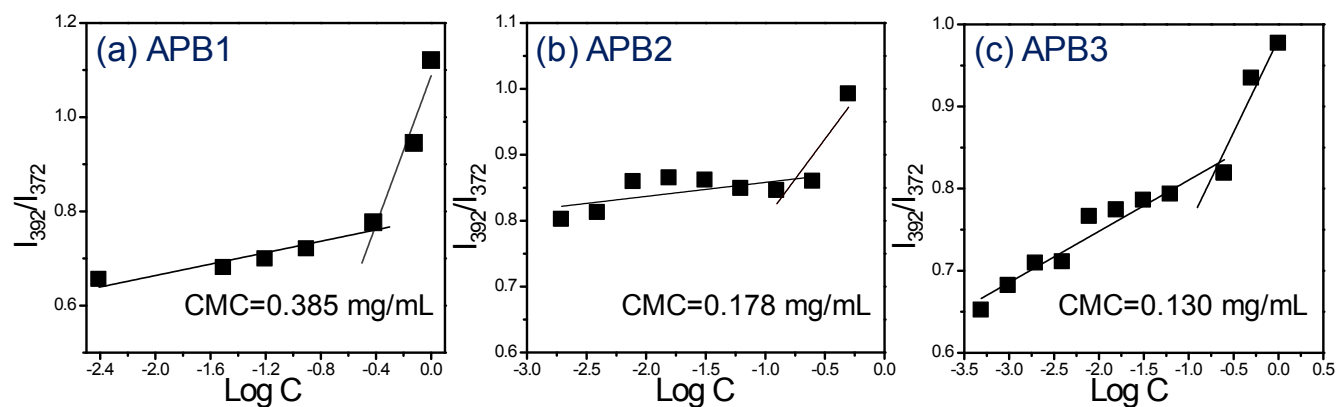
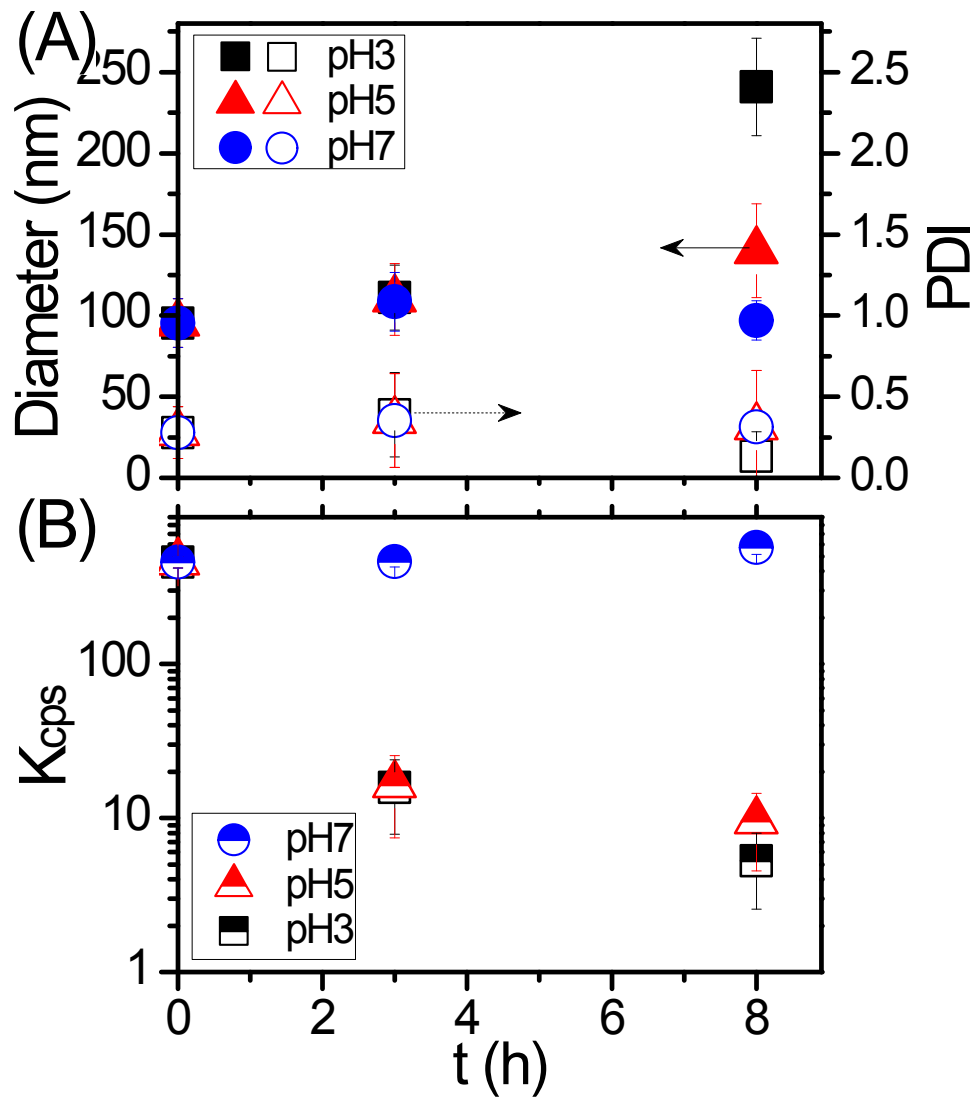


Figure S9. Monitoring the stability of micelles in different pH values and times in RT by DLS.



References:

1. C. F. Huang, S. W. Kuo, D. Moravčíková, J. C. Liao, Y. M. Han, T. H. Lee, P. H. Wang, R. H. Lee, R. C. C. Tsiang and J. Mosnáček, *RSC Adv.*, 2016, **6**, 51816-51822.
2. Y. M. Han, H. H. Chen and C. F. Huang, *Polym. Chem.*, 2015, **6**, 4565-4574.